Membrane actions of RC slabs in mitigating progressive collapse of building structures

Tan Kang Hai[1], **Pham Xuan Dat**[2]

[1] *School of Civil and Environmental Engineering, Nanyang Technological University, Nanyang Avenue, 639798 Singapore* (ckhtan@ntu.edu.sg)
[2] *School of Civil and Environmental Engineering, Nanyang Technological University, Nanyang Avenue, 639798 Singapore* (pham0046@ntu.edu.sg)

Abstract

The potential for progressive collapse of RC buildings can be studied using column loss scenarios. The loss of either internal or external penultimate columns is among the most critical scenarios since the affected beam-and-slab substructure associated with the removed column becomes laterally unrestrained with two discontinuous slab edges. At large deformations, the membrane behaviour of the affected slab, consisting of a compressive ring of concrete around its perimeter and tensile membrane action in the central region, represents an important line of defense against progressive collapse. The reserve capacity can be used to sustain the amplified gravity loads and to mitigate the progressive collapse of building structures. In this paper, an advanced finite model (FEM), which is first verified by available test data, is used to investigate the membrane behavior of RC slabs under the effect of three conditions: The presence of interior beams, rotational restraint along the perimeter edges of the slabs and top reinforcement. It is found that with the presence of interior beams, more tensile membrane forces may be mobilized in the central region as the beam reinforcement is in tension together with slab reinforcement. In the outer region, the compressive ring of concrete which equilibrates the tensile membrane forces may also be strengthened by hogging moment in the top reinforcement along the perimeter edges. These conditions actually enhance the load-carrying capacity of the beam-slab structure to sustain the applied load severely amplified by the doubling-of-span effect due to the loss of a supporting column.

Keywords: Progressive collapse; Penultimate column loss scenarios; Membrane actions; Reinforced concrete slabs; Large deformations; Finite element analysis.

1. Introduction

When a ground column is severely damaged by an explosion, axial compressive force above this column will vanish quickly within a few milliseconds. As a result, all floors above the first floor will deflect identically and dynamically under uniform gravity load to seek a new equilibrium path. The structure may collapse during or after the free vibration phase. There are two significant changes following a column removal:

1. Spans of slabs and beams bridging over the removed column will double the initial ones.
2. Existing gravity loads are amplified by a dynamic factor less than two.

By conducting purely elastic analysis, it is clear that bending moments along the affected beams and slabs are four times the initial values. In addition, these bending moments are proportional to a dynamic factor larger than one. At large vertical displacements, flexural capacities of affected beams and slabs are insufficient to resist these applied loads. Just before the final collapse kicks in, affected beams and slabs may carry the loads with steel reinforcement acting as a kind of tensile net.

Recently, great efforts have been made by the research community to study the behaviour of structures under the loss of columns. Most attention has been devoted to the behaviour of beams bridging over removed columns under amplified gravity loads. It was concluded by Sasani and Kropelnicki (2007), Wei-Jian Yi and Kunnath (2008) that a large reserve capacity of catenary action in beams, which carries applied loads by the tension mode, is crucial to mitigating progressive collapse.

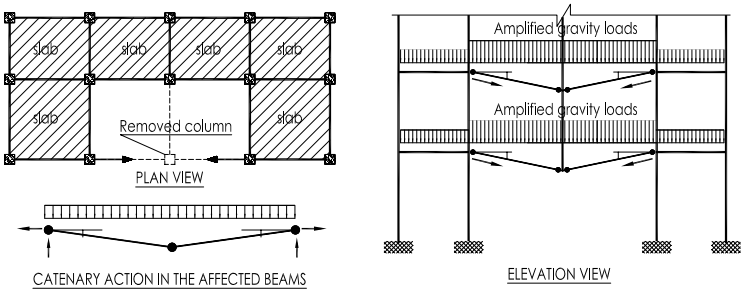

Fig. 1: Catenary action in beams under a loss of an external mid-span column

The shortcoming with relying catenary action in preventing progressive collapse is due to its high demand on lateral restraint. When a mid-span column is removed, adjacent slabs provide sufficient in-plan diaphragm stiffness to support the tension forces, resulting in the development of catenary action (**Fig. 1**). However, when either internal or external penultimate column is removed, the horizontal catenary forces may pull in the external perimeter columns, leading to a partial collapse of the structure. In such a situation, the catenary action may be a cause rather than a prevention of progressive collapse (**Fig. 2**).

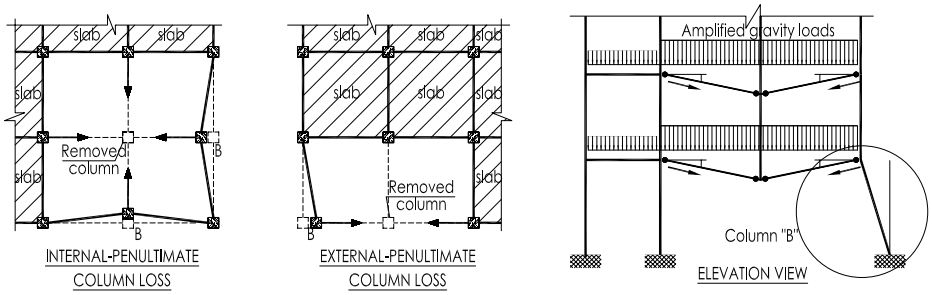

Fig. 2: Instability of perimeter columns ”B” due to horizontal catenary forces

This research focuses on the membrane actions of the affected slab in preventing progressive collapse. Under either external or internal penultimate column loss scenario, the affected slabs become laterally unrestrained with two consecutive edges discontinuous. At large deformations, the RC slabs are capable of forming a peripheral compressive ring which can support the tension forces in the central deflected area. It is envisaged that the peripheral compressive ring will reduce the demand of catenary action on the perimeter columns and therefore the structure can hold up longer before the onset of progressive collapse (**Fig. 3**).

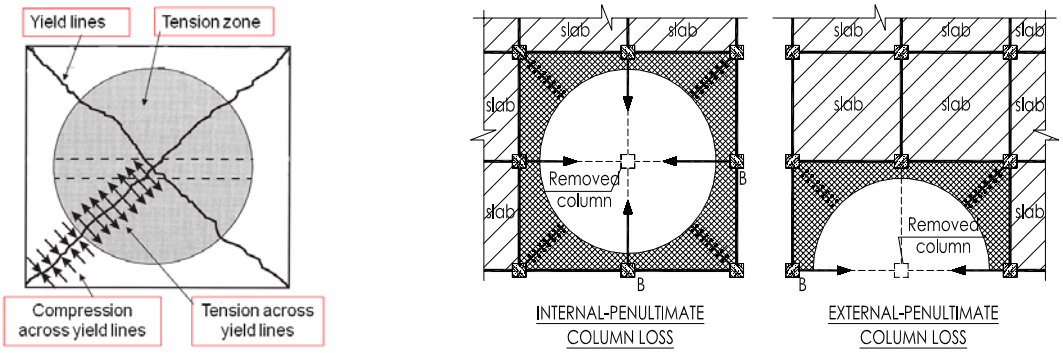

a) Membrane actions in a uniformly loaded slab simply supported all around its edges

b) Membrane actions in slabs under penultimate column loss scenarios

Fig. 3: Membrane actions in a simply supported slab and in beam-slab structures

Membrane actions in a laterally unrestrained slab can be explained by **Fig. 3(a)**. After the formation of yield lines, the slab is divided into four independent parts which are connected together by the yield lines. At large deformations the independent parts tend to move inwards under the action of increasing tensile forces at the centre of the slab, but are restrained from doing so by adjacent parts, creating a peripheral ring of compression supporting the central net of tensile forces. The load-carrying capacity therefore comprises tensile membrane action in the centre of the slab and increasing yield moment in the outer ring where in-plane compressive stresses occur.

The behaviour of laterally unrestrained slabs at large deformations has been extensively studied by Hayes, Sawczuk (1965); Brotchie and Holley (1971) and Mitchel *et. al.*(1984). It has been shown that the load-carrying capacity of TMA was at least twice the yield-line capacity. Recently, these mechanisms have been successfully applied to prevent collapse of composite floors subjected to compartment fires in Europe through a simplified design method developed by Bailey *et al* (2000).

The similarity between a simply-supported slab which has been extensively investigated and a typical affected beam-slab structure associated with a penultimate column loss is the laterally-unrestrained boundary condition since two adjacent perimeter edges are free to move horizontally. The main differences in the beam-slab structure from a simply-supported slab are listed as follows:

1. Rotational restraint with top reinforcement is available along the perimeter edges of the slab.
2. Two interior beams are placed at the centre line of the slab.
3. A considerable amount of top reinforcement exists along the interior beams.

Besides, due to the doubling-of-span effect the span-to-depth ratio increases up to 80 compared with 40 times, the maximum for a single panel.

In this paper, a static numerical analysis is conducted to investigate the behaviour of a beam-slab substructure associated with an internal-penultimate column loss scenario. The boundary condition is rotationally restrained but laterally unrestrained; and the vertical applied load is uniformly distributed loads. The non-linear finite element software, DIANA, is used for this purpose. Three additional factors listed above will be added one at a time to an original model, a simply supported slab, to evaluate their contributions to the overall structural behaviour (**Fig. 4**).

2. Finite element analysis

2.1 Numerical case study

A series of reinforced concrete sub-assemblage specimens, referred to as 'PI' series (Penultimate Internal column loss) is designed to study tensile membrane action of beam-slab systems subjected to the column loss scenario. Dimensions of the test specimens are obtained by scaling down to ¼ of a prototype nine-storey building structure (**Table 1**). The prototype building is designed for gravity loading to BS-8110-97, with the design live load of 3 kN/m^2 and the imposed dead load of 2 kN/m^2. Exterior beams are designed for an additional wall load of 1 kN/m.

Table 1: Dimensions of structural elements

Dimensions	The prototype building	The test specimens
Beam section (WxD)	30 cm x 50 cm	7.5 cm x 12.5 cm
Slab thickness	16 cm	4 cm
Span length	600 cm	150 cm

The main variable studied in this series is the slab reinforcement ratio. There are four specimens with four different reinforcement ratios. For each specimen, the top reinforcement ratio (ρ_{top}) is twice the bottom one ($\rho_{bot.}$) (**Table 2**). Dimensions of all structural elements such as beams, slabs and columns are kept the same in all the numerical specimens.

Table 2: Case studies for Penultimate column loss condition

	ρ_{top} = 0.86% ρ_{bot} = 0.43%	ρ_{top} = 1.14% ρ_{bot} = 0.57%	ρ_{top} = 1.42% ρ_{bot} = 0.71%	ρ_{top} = 1.72% ρ_{bot} = 0.86%
Case 1	IP 11	IP 12	IP 13	IP 14
Case 2	IP 21	IP 22	IP 23	IP 24
Case 3	IP 31	IP 32	IP 33	IP 34
Case 4	IP 41	IP 42	IP 43	IP 44

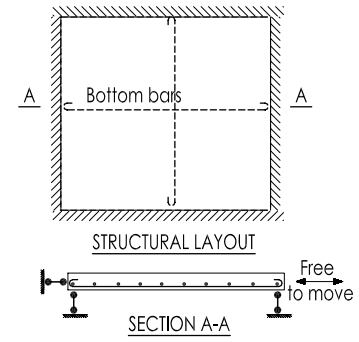

(a) Case 1: A simply supported slab

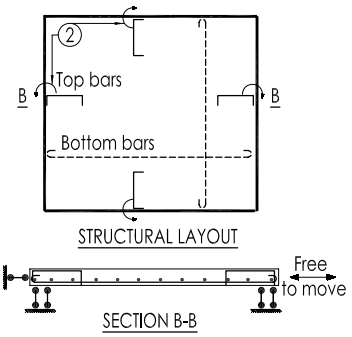

(b) Case 2: A rotationally restrained slab

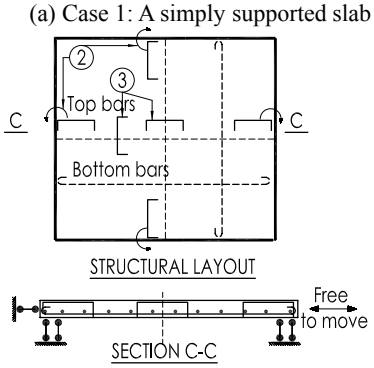

(c) Case 3: A rotationally restrained slab with top bars

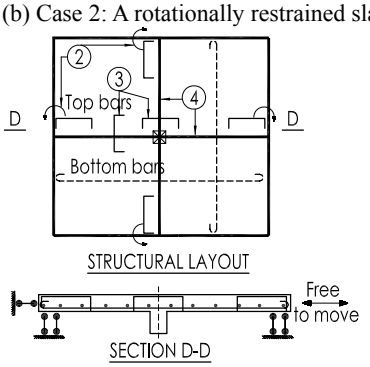

(d) Case 4: A rotationally restrained beam-slab system

Fig. 4: Considered cases in each specimen for estimating the influence of additional factors

2.2 Finite element modelling

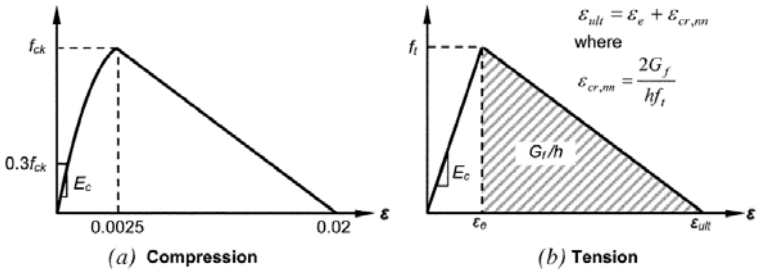

(i) Uniaxial relationship of concrete material

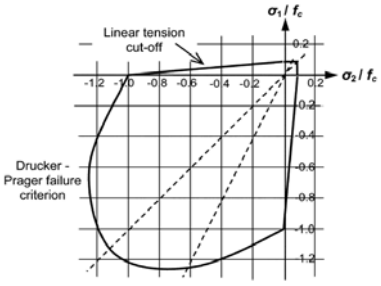

(ii) Biaxial strength of concrete

Fig. 5: Concrete material adopted in this analysis

Fig. 5(i) shows the European CEB-FIP concrete Model Code adopted in this study. The peak compressive strength is defined as the value of the characteristic cylinder-compressive strength f_{ck} and the initial linear elastic stage of the concrete model is up to 30% of the compressive strength.

The constitutive behaviour of concrete under biaxial state of stress is modelled by the Drucker-Prager failure surface as shown in **Fig. 5(ii)**. For concrete in tension, multi-directional fixed smeared crack model which is specified by a combination of tension cut-off, tension softening and shear retention is adopted for concrete in tension. The shear stiffness of concrete material after the formation of cracking is defined with a constant value of 0.2.

The constitutive behaviour of steel reinforcement is modelled by using an elasto-plastic biliniear model. The Von Mises plastic criterion is applied together with the work hardening hypothesis.

Table 3: Material properties

Concrete		Steel reinforcement	
Young modulus E_c	$1.94*10^4$ MPa	Young modulus E_s	$2.1*10^5$ MPa
f_{ck}	33 MPa	f_y	210 MPa
f_t	3.1 MPa	f_u	250 MPa
Fracture energy G_f	0.07 MPa		

The element used to model reinforced concrete beams and slabs is eight-node quadrilateral isoparametric curved layered shell elements (CQ40L) (Fig.6a). The main assumptions of this element are listed follows:

1. Plane sections remain plane but their normal vectors are not necessarily normal to the reference surface. Shear deformation is included in Mindlin-Reissner theory.
2. The shell elements are multi-layered with the normal stress between two adjacent layers reduced to zero. In each layer, the shear strains are constrained by a shear correction factor.

Each element node has five degrees of freedom, viz. three translations and two rotations. Reinforcement in beams and slabs is modelled by planar grid reinforcement embedded in the shell elements, so-called mother elements. Reinforcement strain reachings are computed from the strains of the mother elements with perfect bonding between reinforcement and surrounding concrete material. The thickness of the grid reinforcement is equivalent to the reinforcement area per unit length of structural elements (beams and slabs).

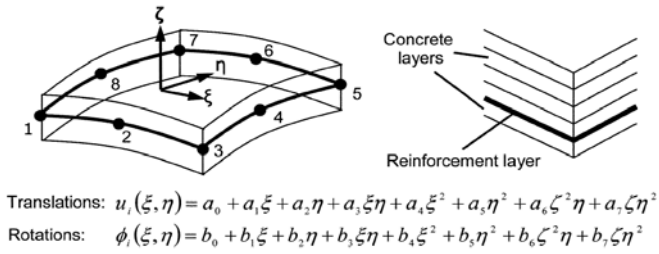

a) The curved layered shell element CQ40L [T1]

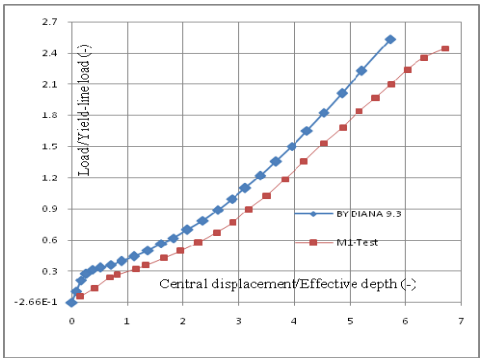

b) Comparison between M1-test and numerical prediction by DIANA 9.3

Fig. 6: Adopted finite element and the verification job

In this analysis, the incremental-iterative solution procedure consisting of two parts: the incremental part and the iteration part is employed to solve the non-linear problem. In the increment part, the displacement field of a nonlinear problem should be divided into many increments using arc-length method. In the iteration part, the equilibrium stage at the end of every increment can be achieved by the regular Newton-Raphson method. The geometrical nonlinear effects are taken into account by Total Lagrangian method for large deformation but small strain problems. The finite elements, material properties and nonlinear analysis procedures are verified through the test M1 conducted by Bailey et al (2008). The slabs are uniformly loaded all round with simply supported boundary condition. A reasonably good correlation between the numerical analysis and test results is obtained as shown in **Fig. 6(b)**.

2.3 Discussion on numerical results

Sixteen cases are analyzed by DIANA in order to investigate the effects of the additional factors on the membrane behaviour of concrete slabs subjected to uniformly distributed loads. The finite element analysis proceeds very well into the membrane stage until termination occurs at the vertical central deformations at about 3 to 5 times the effective depth of slabs. The recorded points of interest are horizontal reactions along the center lines which can represent both tension and compression membrane forces in the slab bodies, moment and vertical reaction forces along the perimeter edges, strain and stress of both concrete and reinforcement materials and vertical displacements of node elements. These points provide valuable insight into the membrane behaviour of concrete slabs at large deformations. Some interesting observations will be discussed as follows.

2.3.1 Development of membrane actions in a simply supported slab

In-plane membrane mechanism, comprising a compressive ring of concrete around the slab perimeter and tensile membrane action in the central region, begins to develop at a central displacement of 35 mm, which is about one effective depth of the slab. As the vertical displacement increases, the central tensile region expands quickly, resulting in greater in-plane membrane forces. At very large displacements, the area of central region and the magnitudes of membrane forces do not change very

much until the analysis terminates due to convergence difficulty.

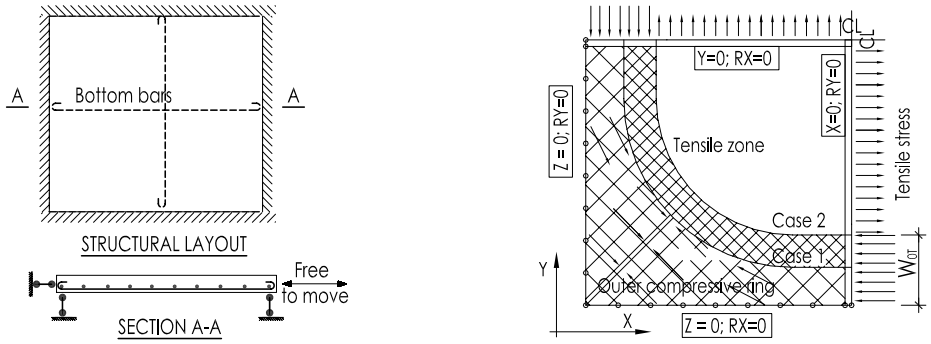

(a) Case 1: A simply supported slab (b) In-plane stress distribution in a quarter

Fig. 7: Membrane actions in a simply supported slab

As shown in **Fig. 7**, the development of membrane actions in slab PI 11 becomes more evident at a displacement of 135 mm. At this displacement, the width of the peripheral compressive ring is about 150 mm, and the magnitude of membrane force is about 63.5 kN. It is noted that the sum of the tension forces in the central region should be equal to that of the compressive force in the peripheral ring at any displacement.

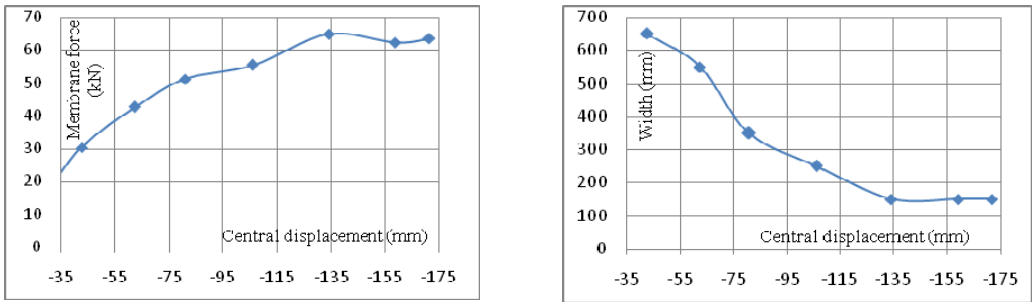

(a) Membrane forces versus central displacement (b) Width of the outer ring versus displacement

Fig. 8: Development of membrane actions in slab PI 11

2.3.2 Membrane actions in a rotationally restrained slab (Case 2)

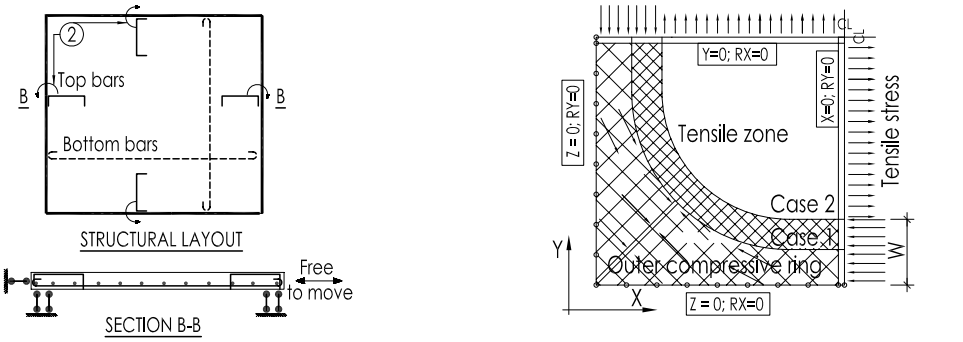

(a) Case 1: A simply supported slab (b) In-plane stress distribution in a slab quarter

Fig. 9: Development of membrane actions in Case 2

Sufficient strength of the outer compressive ring is a vital condition to prevent the progressive collapse of beam-slab structures subjected to a penultimate column loss. Failure of the ring may cause structural collapse as shown in **Fig. 2**.

With rotational restraint and top reinforcement along the perimeter edges of a laterally-unrestrained slab, the presence of hogging moment is obvious. It is found that this moment can strengthen the outer compressive ring by enlarging the width of the ring and redistributing the compressive stress throughout the depth of the slab in this region.

A larger compressive ring means that the size of tensile central region is reduced (**Fig. 4.17 b**). This leads to less tensile membrane force to be mobilized. As shown in **Fig. 10(a)**, the total membrane force

in Case PI 22 (with rotational restraint) is only about 70% of that in PI 12 (without rotational restraint).

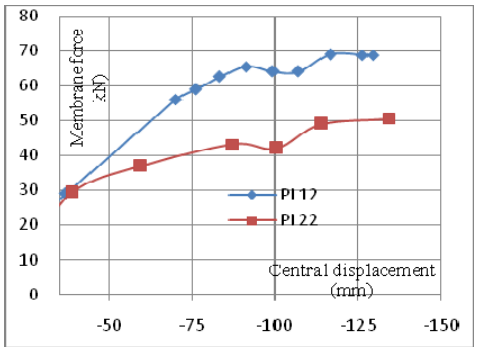

(a) Membrane forces versus central displacement

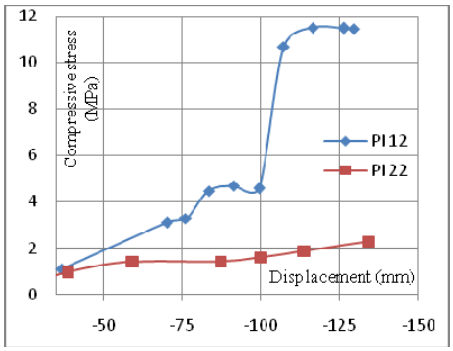

(b) Average compressive stress in the outer ring

Fig. 10: Comparison of predictions between slabs in Case 1 and Case 2

The redistribution of the compressive stress due to the hogging moment along the perimeter edges is highly noticeable. In the cross section of the outer ring at the center line position, the compressive stress can be calculated as follows:

$$\sigma_{comp} = \frac{F}{T * W_{oT}}$$

where: σ_{comp} is the average compressive stress through slab cross section; F is total membrane force; T is thickness of slab and W_{oT} is the width of compressive ring.
Fig. 10(b) shows a significant reduction of the average compressive stress in Case PI 22 compared with Case PI 12.

2.3.3 Membrane actions in a rotationally restrained slabs (Case 3)

Compared with Case 2, top reinforcement is added along the center lines of the slabs. The contribution to the overall load-carrying capacity is not so obvious when the deformation is relatively small as shown in Fig. 13. This can be explained by a low tension stress level in the reinforcement whose maximum value is only 70 N/mm^2, about 30% of yield stress of reinforcement, at a central displacement of 110 mm.

2.3.4 Membrane actions in a rotationally restrained beam-slab system (Case 4)

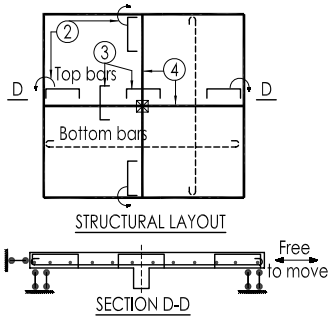

(a) Case 1: A simply supported slab

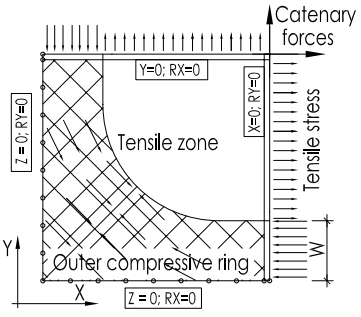

(b) In-plane stress distribution in a quarter

Fig. 11: Comparison of membrane forces and compressive stress between

A full beam-slab structural model (**Fig. 11**) is obtained by adding interior beams into the rotationally restrained slab (Case 3). As expected, interior beams enhance the membrane forces due to an additional amount of reinforcement in tension in the central area. As shown in **Fig. 12(a)**, at a displacement of 135 mm membrane forces in slab PI 42 (with interior beams) nearly double that in slab PI 22 (without beams). Obviously, the compressive stress in slab PI 42 also increases significantly (Fig.12b) but is still lower than that in slab PI 12 with simply supported boundary condition.

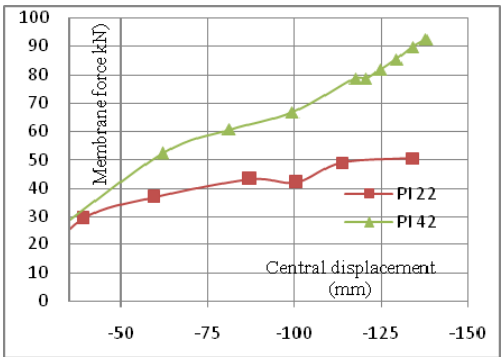

(a) Membrane forces versus central displacement

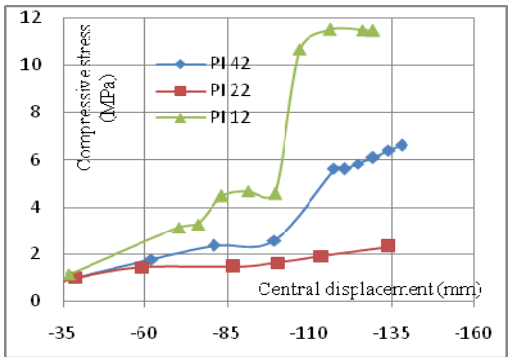

(b) Average compressive stress σ_{comp}

Fig. 12: Membrane forces and compressive stress in Cases 2&4

Pure tensile membrane action which is defined by the presence of tensile strain at the top surface of slabs is observed in all cases. **Table 4** provides the average value of tensile strain in the top and bottom bars of interior beams at the last load step of the finite element analysis. It is evident that the top reinforcement of beams in the central region and the slabs is able to contribute significantly to the tensile membrane force together with the bottom reinforcement.

Table 4: Average strain in the finite elements in the central region

	Slab PI 41	Slab PI 42	Slab PI 43	Slab PI 44
$\varepsilon_{ave\text{-}top}$ (10^{-3})	0.910	0.633	0.456	0.827
$\varepsilon_{ave\text{-}bot}$ (10^{-3})	1.610	1.428	1.358	1.35

2.3.5 Enhancement of the overall load-carrying capacity

Load-displacement predictions in sixteen cases can be shown in Fig.13.

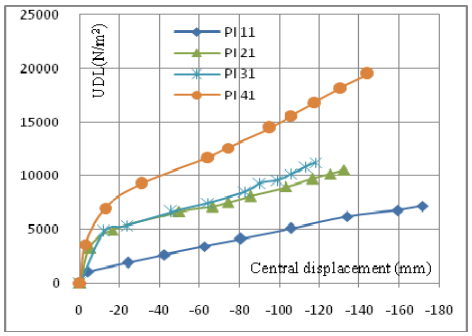

(a) Slab bottom reinforcement Ratio ρ = 0.43%

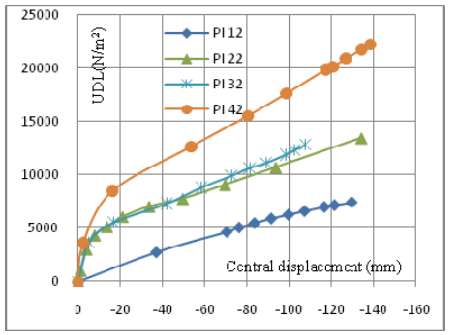

(b) Slab bottom reinforcement Ratio ρ = 0.57%

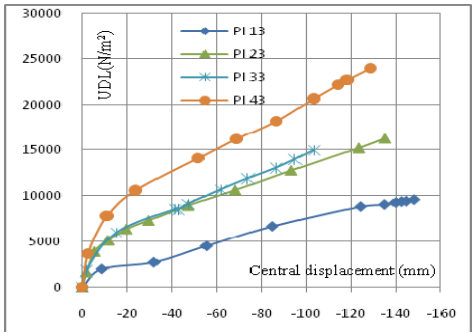

(c) Slab bottom reinforcement Ratio ρ = 0.71%

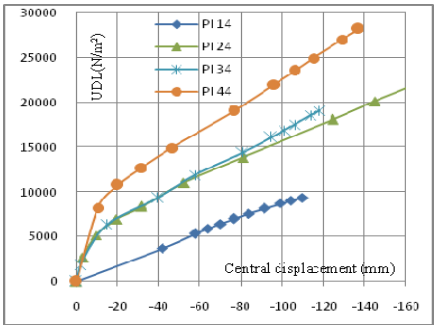

(d) Slab bottom reinforcement Ratio ρ = 0.86%

Fig. 13: Load-displacement curves of slabs enhanced by additional factors

Based on a series of load-displacement curves, the overall load-carrying capacity can be summarized in **Fig. 14**.

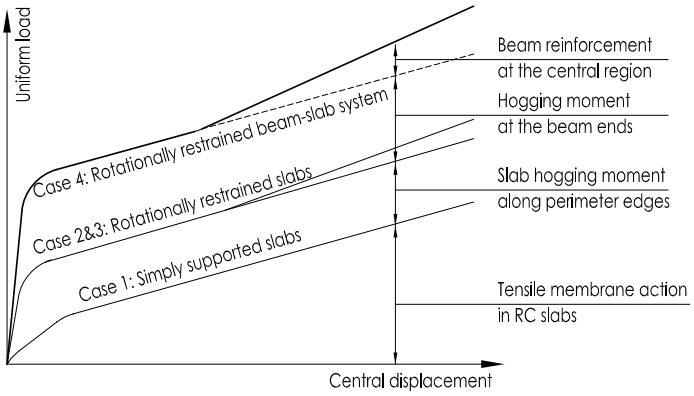

Fig. 14: Partial contributions to the overall load-carrying capacity of beam-and-slab substructures

While tensile membrane capacity is obviously proportional to the vertical displacement, it is of interest that whether flexural capacities of beams and slabs along perimeter edges are significant at large displacements. As shown in **Fig. 15**, as long as termination of the analysis occurs, there is no sign of flexural stiffness degradation of both beams and slabs. This allows for predicting more accurately the overall load-carrying capacity.

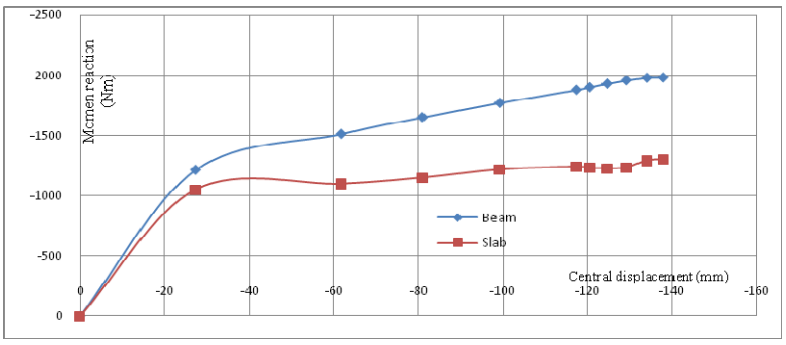

Fig. 15: Moment reaction of beams and slabs along the perimeter edges

2.3.6 Termination of the finite element analysis

In all cases, the FE analysis proceeds far into the pure tensile membrane behaviour. The ultimate displacements obtained in the analysis vary from 171 mm (PI 11) to 107 mm (PI 32). In Case 4 (rotationally-restrained slabs with beams), the termination of analysis is mainly due to excessive compressive concrete crushing larger than the predefined value, which occurs at the bottom surface of interior beams in the negative bending region.

However, it is argued that since membrane actions are more dominant at this stage, the structure is able to sustain higher loads by membrane actions when displacements become larger. In such a situation, the ultimate stage, which is governed by the strength of the compressive ring, is actually beyond the numerical prediction of load-carrying capacity. This is due to the limited success in using DIANA to predict the post-failure behaviour of the models.

3. Conclusions

Internal penultimate column loss is among the most critical scenarios which can result in high potential for progressive collapse since the affected beam-and-slab substructure associated with the removed column becomes laterally unrestrained. As catenary action of beams itself is no longer effective due to the lack of lateral restraint, membrane action in RC slabs with a peripheral compressive ring is the only alternative load path to redistribute the applied loads.

The load-carrying capacity of membrane actions in the affected beam-slab substructures can be greatly enhanced by additional factors such as rotational restraint, interior beams, and negative moment reinforcement of slabs. The contributions of these factors are to be quantified with the highest

contribution from interior beams, rotational restraint and negative moment reinforcement along the interior beams. The enhanced capacity is a key feature to sustain the amplified gravity loads and therefore to mitigate the progressive collapse of building structures.

Although the finite element analysis proceeds very well into the membrane stage in all considered cases, it is still not possible to obtain the failure modes of beam-slab substructures. It requires experimental work to obtain the failure modes. Currently, an experimental programme conducted on ¼ scaled models of the beam-and-slab substructures subjected to large deformations is being prepared in NTU. As shown in **Fig. 16**, the boundary condition of specimens is laterally unrestrained but rotationally restrained. A uniformly distributed load is simulated by twelve loading points equally redistributed from an actuator by means of loading tree.

Fig. 16: A typical setup for beam-slab systems subjected to a penultimate column loss scenario

Acknowledgements

The work presented in this paper is supported by the research funding from Defence Science & Technology Agency (DSTA) titled as: *Effects of catenary and membrane actions on the collapse mechanisms of RC buildings*. The financial support of DSTA is gratefully acknowledged. Sincere thanks are given to Dr Toh Wee Siang for his technical assistance in finite element modelling.

References

[1] Bailey C. G., Wee S. Toh, and Bok M. Chan (2008), *Simplified and advanced analysis of membrane action of concrete slabs*, ACI Structural Journal 105(S04).

[2] Bailey C. B (2001), *Membrane action of unrestrained lightly reinforced concrete slabs at large displacements*, Engineering Structures 23 (2001) 470-483.

[3] Dusenberry D.O. (2000), *Practical means for collapse prevention*, Technical report.

[4] General Services Administration (GSA) (2003), *Progressive Collapse Analysis and Design Guidelines for New Federal Office Buildings and Major Modernization Projects*.

[5] TNO DIANA BV, DIANA *Finite Element Analysis User's Manual Release 9.3*, Delft, the Netherlands, 2008.

[6] Park, R., and Gamble, W. L. (2000), *Reinforced Concrete Slabs*, John Wiley & Sons, Inc.

[7] Dennis Mitchell, and William D. Cook (1984) "Preventing progressive collapse of slab structures" Journal of Structure Engineering 23(07).

[8] Sasani, M., and Kropelnicki, J. (2007) "*Progressive collapse analysis of an RC structure*" The Structural Design of Tall and Special Buildings.

[9] Wei-Jian Yi, Qing-Feng He, Yan Xiao, and Sashi K.Kunnath (2008) "*Experimental study on progressive collapse-resistant behaviour of reinforced concrete frame structures*" ACI Structural Journal 105(4).